

# Polymerization of Phenylacetylenes Using Rhodium Catalysts Coordinated by Norbornadiene Linked to a Phosphino or Amino Group

Naoya Onishi,<sup>†</sup> Masashi Shiotsuki,<sup>\*,‡</sup> Toshio Masuda,<sup>§</sup> Natsuhiko Sano,<sup>⊥</sup> and Fumio Sanda<sup>\*,†</sup>

<sup>†</sup>Department of Polymer Chemistry, Graduate School of Engineering, Kyoto University, Katsura Campus, Nishikyo-ku, Kyoto 615-8510, Japan

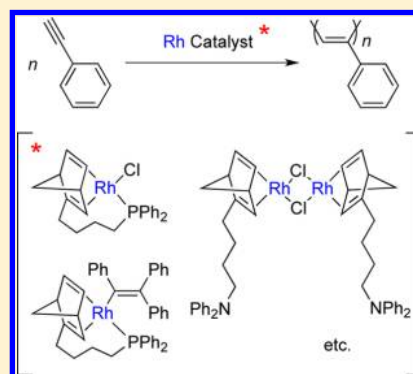
<sup>‡</sup>Molecular Engineering Institute, Kinki University, Kayanomori, Iizuka, Fukuoka 820-8555, Japan

<sup>§</sup>Department of Environmental and Biological Chemistry, Faculty of Engineering, Fukui University of Technology, 3-6-1 Gakuen, Fukui 910-8505, Japan

<sup>⊥</sup>R&D Division, Nippon Chemical Industrial Co., Ltd., 11-1, 9-Chome, Kameido, Koto-ku, Tokyo 136-8515, Japan

## Supporting Information

**ABSTRACT:** The novel rhodium (Rh) catalysts  $[\{\text{nbd}-(\text{CH}_2)_4\text{-X}\}\text{RhR}]$  (**1**, X = PPh<sub>2</sub>, R = Cl; **2**, X = NPh<sub>2</sub>, R = Cl; **3**, X = PPh<sub>2</sub>, R = triphenylvinyl; nbd = 2,5-norbornadiene) were synthesized, and their catalytic activities were examined for the polymerization of phenylacetylene (PA) and its derivatives. Rh-103 NMR spectroscopy together with DFT calculations (B3LYP/6-31G\*-LANL2DZ) indicated that catalyst **1** exists in a mononuclear 16-electron state, while **2** exists in dinuclear states. Catalyst **1** converted PA less than 1% in the absence of triethylamine (Et<sub>3</sub>N). Addition of Et<sub>3</sub>N and extension of the polymerization time enhanced the monomer conversion. On the other hand, catalysts **2** and **3** quantitatively converted PA in the absence of Et<sub>3</sub>N to afford the polymer in good yields. Catalyst **3** achieved two-stage polymerization of PA.



## INTRODUCTION

Substituted polyacetylenes have received considerable attention due to the useful properties resulting from their stiff  $\pi$ -conjugated main chains, including photoconductivity, electroluminescence, and gas permeability.<sup>1</sup> They are commonly synthesized by polymerization of the corresponding monomers catalyzed by transition-metal complexes, with rhodium (Rh) catalysts being the most widely used, due to their high functional-group tolerance and cis stereoregularity of the main chains of the resulting polymers. Most Rh catalysts for acetylene polymerization contain a bicyclic diene ligand such as 2,5-norbornadiene (nbd), because of the high stability of the rigidly chelated structures. Masuda and co-workers have reported that the  $\pi$ -acidity of bicyclic diene ligands largely affects the catalytic activity of Rh catalysts.<sup>2</sup> For example, Rh catalysts bearing the highly  $\pi$ -acidic tetrafluorobenzobarrelene (tfb) ligand polymerize acetylene monomers much more quickly than their nbd counterparts. The high  $\pi$ -acidity of the tfb ligand induces a considerable back-donation from filled 4d orbitals of Rh to the LUMO of tfb, resulting in a more facile coordination of a monomer to the Rh center. Thus, it is expected that more sophisticated bicyclic diene ligands may further improve catalytic activity.

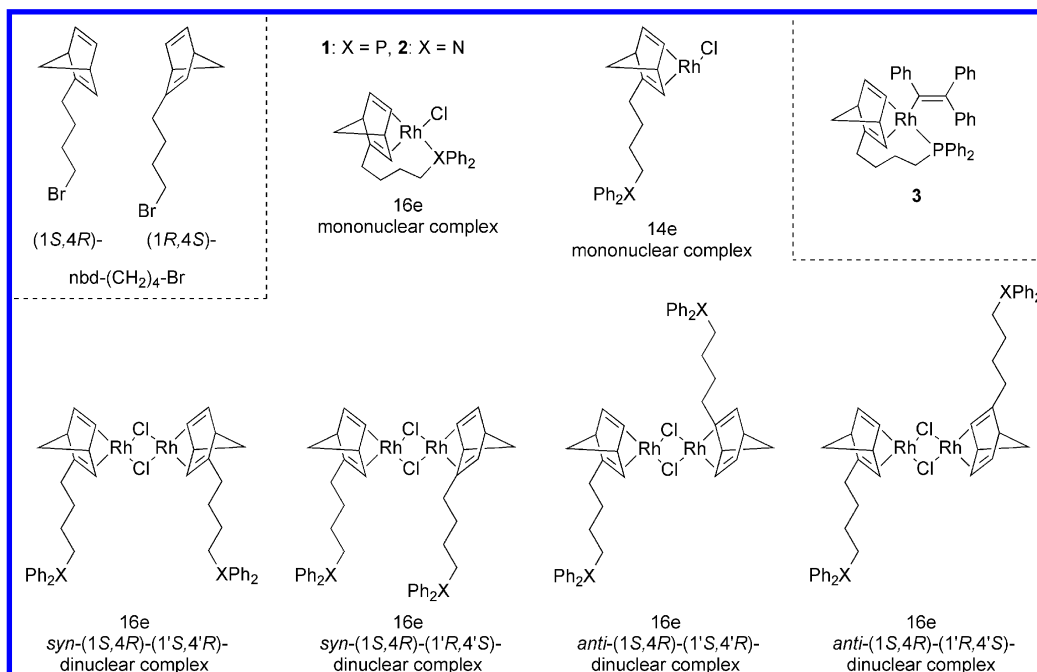
One method for the synthesis of substituted bicyclic diene ligands is the Diels–Alder reaction of dienes and/or

dienophiles bearing target substituents. However, substitution on the reagents sometimes causes unsuccessful results in the Diels–Alder reaction due to steric hindrance.<sup>3</sup> Another method for the preparation of modified bicyclic diene ligands is direct introduction of functional groups on dienes. nbd derivatives linked to a phosphino or amino group by  $(\text{CH}_2)_4$  can be synthesized from  $\text{nbd}-(\text{CH}_2)_4\text{-Br}$  (Scheme 1), which is prepared by the reaction of nbd and  $\text{Br}-(\text{CH}_2)_4\text{-Br}$ .<sup>4</sup> This synthetic method allows the introduction of functional groups on nbd by substitution of the bromo group with nucleophiles, leading to easy synthesis of nbd derivatives linked to various functional groups. In particular, a Rh catalyst bearing the triphenylvinyl group,  $[(\text{nbd})\text{Rh}\{\text{C}(\text{Ph})=\text{CPh}_2\}\{\text{P}(\text{4-F-C}_6\text{H}_4)_3\}]$ , polymerizes phenylacetylene (PA) in a controlled fashion.<sup>5</sup> The polymerization is initiated quantitatively by insertion of the triple bond of the monomer between the Rh center and a vinylic carbon atom.

In the present study, we report the synthesis of novel Rh catalysts **1** and **2** coordinated by nbd derivatives bearing phosphino/amino groups, characterization of the structures by <sup>103</sup>Rh NMR spectroscopy, and polymerization of PA with **1** and **2**. We also transformed catalyst **1** into **3**, bearing a

Received: November 27, 2012

Published: January 24, 2013

Scheme 1. Structures of  $\text{nb}d\text{-(CH}_2\text{)}_4\text{-Br}$  and Rh Complexes 1–3

triphenylvinyl group, and studied the polymerization behavior using **3**. The paper discusses the mechanistic aspects of the polymerization on the basis of DFT calculations. As far as we know, catalyst **3** is the first well-defined Rh complex with a tridentate ligand enabling polymerization of substituted acetylene monomers.

## RESULTS AND DISCUSSION

**Synthesis of Novel Rh Complexes 1–3.** Novel *nbd* derivatives bearing  $\text{-(CH}_2\text{)}_4\text{PPh}_2$  and  $\text{-(CH}_2\text{)}_4\text{NPh}_2$  were synthesized by the reaction of  $\text{nb}d\text{-(CH}_2\text{)}_4\text{-Br}$  with the corresponding phosphine and amine derivatives, respectively, in moderate yields. The structures were confirmed by  $^1\text{H}$  and  $^{13}\text{C}$  NMR spectroscopy and elemental analysis. The resulting compounds were reacted with  $[(\text{C}_2\text{H}_4)_2\text{RhCl}]_2$  in  $\text{CH}_2\text{Cl}_2$  to afford complexes **1** and **2**,<sup>2c</sup> as racemic mixtures. In the  $^1\text{H}$  NMR spectra, olefinic proton signals assignable to the olefin moieties appeared around 6.7 and 6.0 ppm, which shifted 3–4 ppm upfield in comparison to those of the dienes before the reaction, due to coordination to the Rh center.

Complex **1** was converted into **3**, which bears the  $\text{-C(Ph)=CPh}_2$  group by the reaction with  $[\text{BrMg}\{\text{C(Ph)=CPh}_2\}]$ , by a synthesis similar to that for other Rh-C(Ph)=CPh<sub>2</sub> complexes.<sup>2a,5,6</sup> It is expected that **3** enables controlled polymerization of PA, because the structure is analogous to the propagating species in acetylene polymerization. Figure 1 shows the ORTEP structure of **3** obtained by single-crystal X-ray analysis. The  $\text{-(CH}_2\text{)}_4\text{-PPh}_2$  group coordinates to the Rh center, as expected. We also tried unsuccessfully to synthesize a Rh-C(Ph)=CPh<sub>2</sub> complex from **2**.

Rh-103 NMR spectra of complexes **1** and **2** were measured in  $\text{CD}_2\text{Cl}_2$  together with that of  $[(\text{nbd})\text{RhCl}]_2$ . The last compound exhibited one signal at  $-7056.9$  ppm, while complex **1** exhibited two signals (Figure 2). These two resonances are assignable to a doublet at  $-7748.2$  ppm with  $J_{\text{Rh-P}} = 166$  Hz, because the  $^{31}\text{P}$  NMR spectrum shows a doublet coupled with Rh with the same coupling constant. On the other hand,

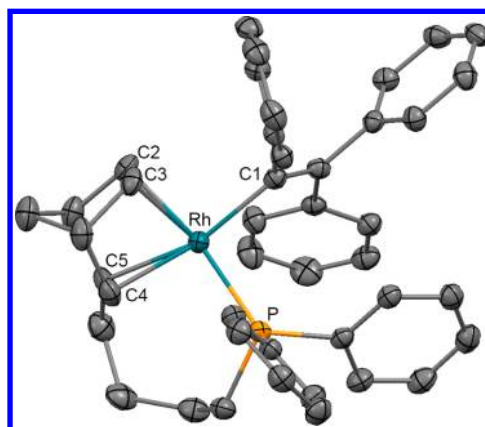


**Figure 1.** ORTEP drawing of the molecular structure of **3** (50% probability ellipsoids). Selected bond distances (Å) and angles (deg): Rh–C1 = 2.062, Rh–C2 = 2.169, Rh–C3 = 2.161, Rh–C4 = 2.223, Rh–C5 = 2.229, Rh–P = 2.288; C2–Rh–C5 = 66.68, C3–Rh–C4 = 65.50, C1–Rh–P = 94.64.

complex **2** exhibited two singlet signals at  $-7051.9$  and  $-7089.7$  ppm ( $\Delta = 476$  Hz)<sup>7</sup> with an integration ratio of 1.1:1. Contamination by a Rh-containing impurity is very unlikely, because the elemental analysis matches the calculated value with an error  $\leq 0.06\%$ .

Various isomeric structures are possible for complex **2** due to the readily dissociative amine of the tridentate ligand. As shown in Scheme 1, one isomer is a 16-electron (16e) complex coordinated by the diene and amino groups. The second one is a 14-electron (14e) complex coordinated by the diene only. There are also several possible dinuclear 16e complexes, possibly consisting of *syn*-(1S,4R)-(1'S,4'R), *syn*-(1S,4R)-(1'R,4'S), *syn*-(1R,4S)-(1'R,4'S), *anti*-(1S,4R)-(1'S,4'R), *anti*-(1S,4R)-(1'R,4'S), and *anti*-(1R,4S)-(1'R,4'S) isomers. It is considered that the complexes are transformable and are in equilibrium in the solution state. We also examined the  $^1\text{H}$

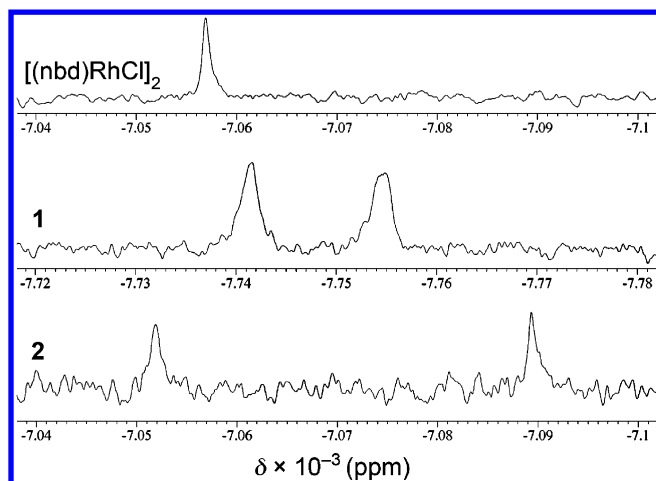


**Figure 2.**  $^{103}\text{Rh}$  NMR (12.6 MHz) spectra of  $[(\text{nbd})\text{RhCl}]_2$ , **1**, and **2** measured in  $\text{CD}_2\text{Cl}_2$ .

NMR spectrum of **2** but could not obtain clear information about the isomers.

According to DFT calculations, the mononuclear 16e complex of **1** is more stable than the mononuclear 14e isomer by 76.3 and 62.1 kJ/mol in enthalpy ( $H$ ) and Gibbs free energy ( $G$ ) in  $\text{CH}_2\text{Cl}_2$ , respectively (Table 1). All *syn*- and *anti*-dinuclear 16e complexes of **1** are energetically unfavorable in comparison with the mononuclear 16e complex, indicating that **1** exists as a mononuclear 16e complex ligated by  $\text{PPh}_2$ , as observed by  $^{103}\text{Rh}$  and  $^{31}\text{P}$  NMR spectroscopy. The presence of a 14e complex is also unlikely, judging from the energy values that are much higher than those of the 16e mononuclear complex. On the other hand, the mononuclear 16e complex of **2** is less stable than the mononuclear 14e isomer by 10.0 and 28.3 kJ/mol in  $H$  and  $G$ , respectively, in  $\text{CH}_2\text{Cl}_2$ . Similar trends are observed in THF. These calculation results provide evidence of the less stable chelation of complex **2**, which contains an amino group, in comparison to complex **1** having a phosphino group. The entropy ( $S$ ) gains by dechelation are  $(4.76\text{--}6.13) \times 10^{-2}$  kJ/(mol K) in  $\text{CH}_2\text{Cl}_2$ , indicating that the

flexibility of the mononuclear 14e complexes is larger than that of the mononuclear 16e counterparts. The Rh–N interatomic distance of **2** (16e, mononuclear) is 2.39 Å in  $\text{CH}_2\text{Cl}_2$  (Table 2). This value is somewhat longer than the Rh–P distance of **1**

**Table 2.** Interatomic Distances between Rh and P/N of **1** and **2** at Mononuclear 16e and 14e States Calculated by the DFT Method (B3LYP/6-31G\*-LANL2DZ)<sup>a</sup>

complex	interatomic distance between Rh and P/N (Å)		
	no solvent	in $\text{CH}_2\text{Cl}_2^b$	in THF <sup>b</sup>
<b>1</b> (16e) mononuclear	2.44	2.34	2.35
<b>1</b> (14e) mononuclear	7.88	7.86	7.86
<b>2</b> (16e) mononuclear	2.52	2.39	2.39
<b>2</b> (14e) mononuclear	7.44	7.50	7.50
<b>3</b> (16e)	2.39	2.40	2.40
<b>3A</b> (14e)	8.78	8.67	8.67

<sup>a</sup>Basis sets: 6-31G\* for C, H, N, P, and Cl; LANL2DZ for Rh. <sup>b</sup>SCRF-IEFPCM method.

(16e, mononuclear) (2.34 Å), even though the van der Waals radius of nitrogen (1.55 Å) is smaller than that of phosphorus (1.80 Å). The lower stability of the nitrogen complex may be responsible for the unsuccessful preparation of the nitrogen analogue of **3** mentioned above. It should be noted that the dinuclear 16e complexes of **2** are energetically much more favorable than the mononuclear 16e complex ( $\Delta H$ , ranging from  $-69.9$  to  $-85.0$  kJ/mol;  $\Delta G$ , ranging from  $-61.5$  to  $-79.0$  kJ/mol). It is very likely that complex **2** exists in dinuclear forms, exhibiting  $^{103}\text{Rh}$  NMR chemical shifts very close to that of  $[(\text{nbd})\text{RhCl}]_2$  in  $\text{CD}_2\text{Cl}_2$ , as shown in Figure 2. The two  $^{103}\text{Rh}$  NMR signals are assignable to *syn* and *anti* isomers and/or isomers with various combinations of (1*S*,4*R*)- and (1*R*,4*S*)-nbd derivatives.

The energy differences between the 16e and 14e complexes of **3** are small ( $\Delta H$ , from  $+15.2$  to  $+18.3$  kJ/mol;  $\Delta G$ , from  $-1.6$  to  $-7.3$  kJ/mol) in comparison with those between the mononuclear 16e and 14e complexes of **1** ( $\Delta H$ , from  $+75.7$  to  $+92.5$  kJ/mol;  $\Delta G$ , from  $+59.9$  to  $+72.8$  kJ/mol). The 14e state (**3A**) seems to be stabilized by the triphenylvinyl group, which

**Table 1.** Relative Energies of Various Possible Complexes of **1**–**3** Calculated by the DFT Method (B3LYP/6-31G\*-LANL2DZ)<sup>a</sup>

complex	energy difference (kJ/mol)					
	no solvent		in $\text{CH}_2\text{Cl}_2^b$		in THF <sup>b</sup>	
	$\Delta H$	$\Delta G^c$	$\Delta H$	$\Delta G^c$	$\Delta H$	$\Delta G^c$
<b>1</b> (16e) mononuclear	0.0	0.0	0.0	0.0	0.0	0.0
<b>1</b> (16e) <i>syn</i> -(1 <i>S</i> ,4 <i>R</i> )-(1' <i>S</i> ,4' <i>R</i> ) dinuclear	+12.2	+24.7	+28.3	+42.8	+26.2	+39.3
<b>1</b> (16e) <i>syn</i> -(1 <i>S</i> ,4 <i>R</i> )-(1' <i>R</i> ,4' <i>S</i> ) dinuclear	+12.0	+23.7	+28.1	+41.6	+26.0	+37.5
<b>1</b> (16e) <i>anti</i> -(1 <i>S</i> ,4 <i>R</i> )-(1' <i>S</i> ,4' <i>R</i> ) dinuclear	+12.1	+22.9	+28.8	+41.9	+26.7	+38.5
<b>1</b> (16e) <i>anti</i> -(1 <i>S</i> ,4 <i>R</i> )-(1' <i>R</i> ,4' <i>S</i> ) dinuclear	+12.4	+20.9	+26.5	+47.9	+24.4	+44.6
<b>1</b> (14e) mononuclear	+92.5	+72.8	+76.3	+62.1	+75.7	+59.9
<b>2</b> (16e) mononuclear	0.0	0.0	0.0	0.0	0.0	0.0
<b>2</b> (16e) <i>syn</i> -(1 <i>S</i> ,4 <i>R</i> )-(1' <i>S</i> ,4' <i>R</i> ) dinuclear	-84.9	-77.6	-70.3	-63.2	-71.1	-63.5
<b>2</b> (16e) <i>syn</i> -(1 <i>S</i> ,4 <i>R</i> )-(1' <i>R</i> ,4' <i>S</i> ) dinuclear	-84.8	-79.0	-70.1	-63.0	-71.0	-64.2
<b>2</b> (16e) <i>anti</i> -(1 <i>S</i> ,4 <i>R</i> )-(1' <i>S</i> ,4' <i>R</i> ) dinuclear	-84.7	-77.5	-69.9	-61.5	-70.7	-62.5
<b>2</b> (16e) <i>anti</i> -(1 <i>S</i> ,4 <i>R</i> )-(1' <i>R</i> ,4' <i>S</i> ) dinuclear	-85.0	-78.6	-70.4	-62.3	-71.2	-63.4
<b>2</b> (14e) mononuclear	+7.9	-10.1	-10.0	-28.3	-9.6	-25.4
<b>3</b> (16e)	0.0	0.0	0.0	0.0	0.0	0.0
<b>3A</b> (14e)	+18.3	-1.6	+15.2	-7.2	+15.2	-7.3

<sup>a</sup>Basis sets: 6-31G\* for C, H, N, P, and Cl; LANL2DZ for Rh. Energy standard: 16e mononuclear complex of each compound. The energy values of dinuclear complexes are divided by 2. <sup>b</sup>SCRF-IEFPCM method. <sup>c</sup>At 298.15 K and 1 atm.

has electron-donating ability, and overlap of the  $\pi$  orbital of one  $\beta$ -phenyl group with the Rh d orbital, as discussed later in this paper.

**Polymerization.** The polymerization of PA was carried out by using catalysts 1–3 (Scheme 2). Catalyst 1 bearing a

**Scheme 2. Polymerization of PA with Rh Catalysts 1–3**

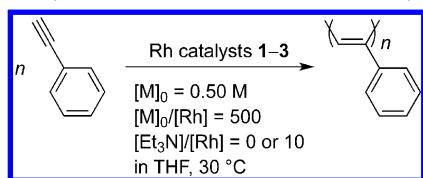


**Table 3. Polymerization of PA with Rh Catalysts 1–3<sup>a</sup>**

run	catalyst	additive	time (h)	conversion <sup>b</sup> (%)	polymer		
					yield <sup>c</sup> (%)	$M_n^d$	$M_w/M_n^d$
1	1	none	24	<1			
2	1	Et <sub>3</sub> N	24	11			
3	1	Et <sub>3</sub> N	72	70	67	69,000	1.7
4	2	none	24	100	83	240,000	1.7
5	3	none	24	100	94	85,000	1.3

<sup>a</sup>Conditions:  $[M]_0 = 0.50$  M,  $[M]_0/[Rh] = 500$ ,  $[Et_3N]/[Rh] = 0$  or 10 in THF at 30 °C. <sup>b</sup>Determined by GC (*tert*-butylbenzene) = 50 mM as an internal standard). <sup>c</sup>MeOH-insoluble part. <sup>d</sup>Estimated by SEC (polystyrene standard).

phosphino group gave less than 1% conversion of the monomer (Table 3, run 1), indicating very low catalytic activity. The monomer conversion increased to 11% when Et<sub>3</sub>N was added as a cocatalyst (run 2). Extension of polymerization time from 24 to 72 h enhanced the monomer conversion to afford the polymer with an  $M_n$  value of 69,000 in a moderate yield (67%) (run 3). On the other hand, catalyst 2 bearing an amino group quantitatively converted PA under the same conditions as those of run 1 to afford the polymer in 83% yield (run 4). The vinyl type complex 3 converted PA quantitatively to give a polymer in 94% yield (run 5). The molecular weight distribution was narrow ( $M_w/M_n = 1.3$ ), in comparison to that for the polymers obtained by the polymerization using 1 and 2 ( $M_w/M_n = 1.7$ ).

The difference in catalytic activities of 1–3 is considered as follows. The amino group of 2 seems to induce the formation of an active 14e mononuclear complex by coordinating to the Rh center of a dinuclear complex in a manner similar to that for Et<sub>3</sub>N in the  $[(nbd)RhCl]_2/Et_3N$  catalyst system.<sup>8</sup> It is likely that the population of this active species is small, because the initiation efficiency is calculated to be as small as 21% (run 4 in Table 3). In contrast, both complexes 1 and 3 exist as mononuclear states. In the case of 3, a PA molecule is smoothly inserted between the Rh and the triphenylvinyl group, resulting in polymerization. On the other hand, some prereactions such as formation of Rh–C≡CPh species are necessary to form an initiating species in the case of 1. As a result, 3 is much more active than 1, even though both catalysts contain a phosphine ligand.

The monomer conversion/time relationship was monitored by GC in order to obtain further information about vinyl catalyst 3 (Figure 3). The monomer conversion reached 100% at 180 min. The first-order plot was nonlinear in the early stage and became linear after about 80 min. After complete monomer consumption, the second portion of PA was fed to the reaction

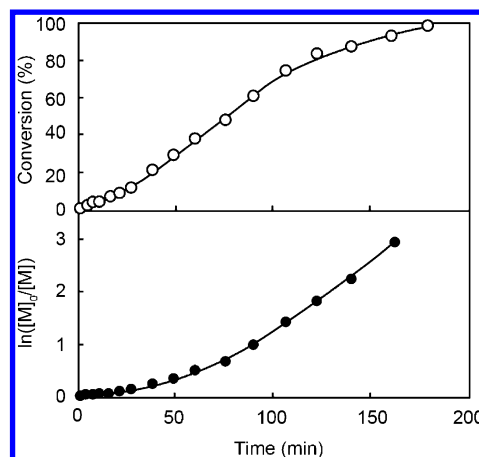


**Figure 3.** Conversion/time and first-order plots for the polymerization of PA with Rh catalyst 3. Conditions:  $[M]_0 = 0.50$  M,  $[M]_0/[Rh] = 500$  in THF at 30 °C.

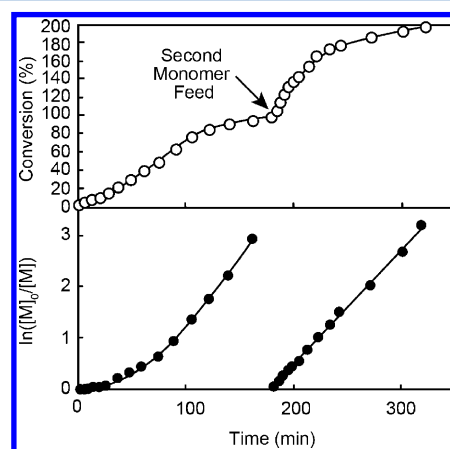


**Figure 4.** Conversion/time and first-order plots for the polymerization of PA after the first and second feeds with Rh catalyst 3. Conditions:  $[M]_0 = [M]_{\text{second}} = 0.50$  M,  $[M]_0/[Rh] = 500$  in THF at 30 °C.

mixture. The polymerization again occurred satisfactorily to convert the second monomer feed quantitatively (Figure 4). Interestingly, the first-order plot was linear during the polymerization after the second monomer feed. The reason for these results is discussed later in this paper.

**Mechanism of Polymerization.** Scheme 3 and Figure 5 depict a plausible mechanism for the polymerization of PA catalyzed by Rh complex 3 and the potential map for the pathway, respectively.<sup>9</sup> The energies were determined by DFT calculations performed in the presence of a solvent (THF) by placing the solute in a cavity within the solvent reaction field.<sup>10</sup> In the present study, we considered the coordination–insertion pathway to give *cis*-*transoidal* poly(PA), which was confirmed by a <sup>13</sup>C labeling study by Noyori and co-workers for Rh-catalyzed PA polymerization<sup>11</sup> and supported by a detailed DFT study by Morokuma and co-workers.<sup>12</sup> First, the phosphine moiety of 16e complex 3 is dissociated from the Rh center to form the 14e complex 3A, having a vacant site. This process is unfavorable regarding  $\Delta H$  (+15.2 kJ/mol) while favorable regarding  $\Delta G$  (−7.3 kJ/mol), likely due to the entropy gain by dissociation of the PPh<sub>2</sub> group from the Rh center. As mentioned above, the analogous transformation from the 16e to 14e complex of 1 is largely endothermic both in  $\Delta H$  and  $\Delta G$ . This difference is explainable by the through-space

Scheme 3. Plausible Mechanism for the Polymerization of PA by Rh Vinyl Catalyst 3

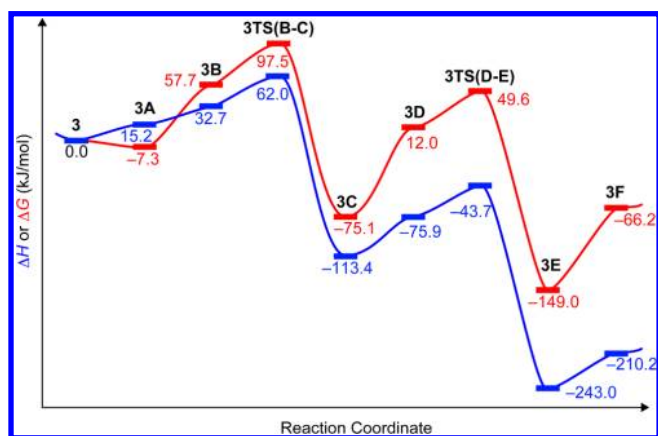
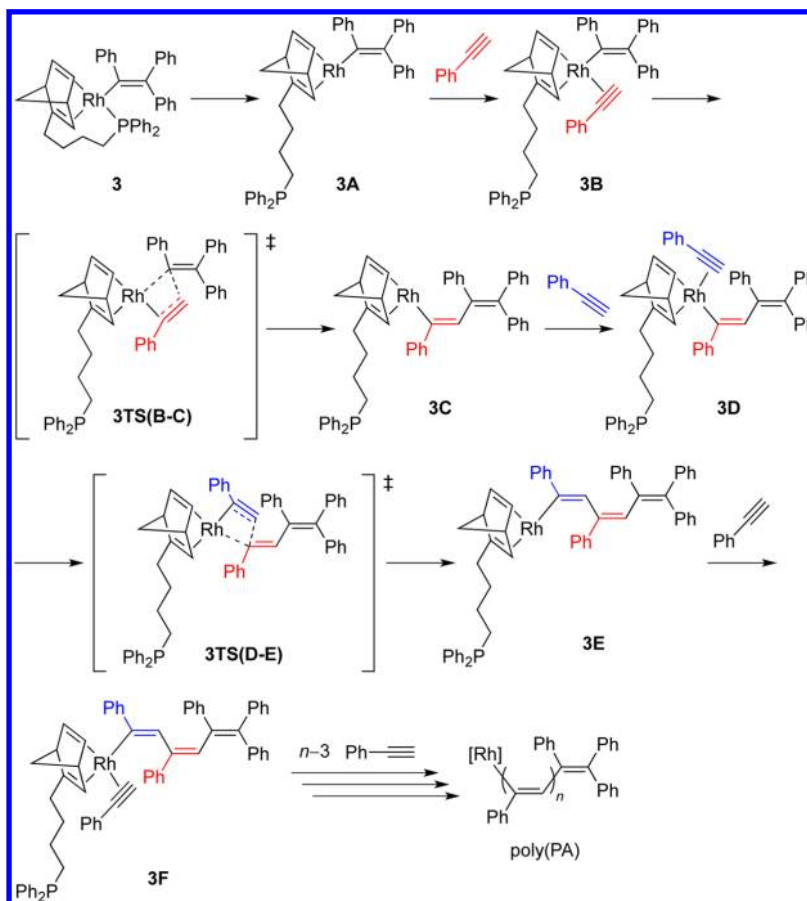


**Figure 5.** Potential map for Scheme 3 illustrated using the  $H$  (blue line) and  $G$  values (red line) of 3 as standards, calculated by B3LYP/6-31G\*-LANL2DZ using SCRF-IEFPCM (solvent THF). The sums with three molecules of PA (3, 3A), two molecules of PA (3B, 3TS(B-C), 3C), and one molecule of PA (3D, 3TS(D-E), 3E) were used to adjust the total atom numbers of the intermediates.

electron donation from the phenyl group of 3A to the Rh center. Namely, the  $\pi$  orbital of one  $\beta$ -phenyl group of 3A overlaps with the Rh d orbital at the vacant site to stabilize the conformer, as shown in Figure 6, left. The overlap of the Rh d orbital with the  $\pi$  orbital of nbd is observed as well, leading to effective stabilization by nbd-Rh-Ph electron delocalization.

Next, a PA molecule (red) is coordinated to the Rh center at the vacant site to give 3B. This step is also endothermic, and in

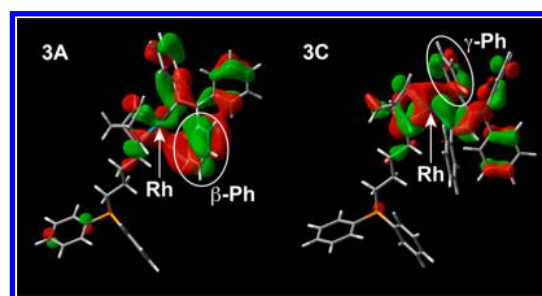
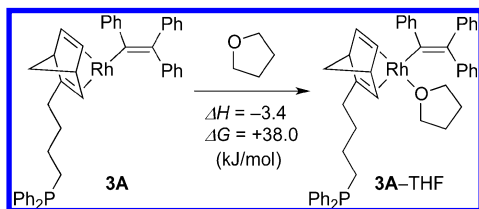


**Figure 6.** Overlap of the Rh (blue) d and phenyl  $\pi$  orbitals of 3A and 3C: (left) with the  $\beta$ -phenyl group of 3A, MO 151; (right) with the  $\gamma$ -phenyl group of 3C, MO 186. Geometries were fully optimized by B3LYP/6-31G\*-LANL2DZ using SCRF-IEFPCM (solvent THF). The red and green parts represent MO surfaces.

this step  $\Delta G$  is also positive (+65.0 kJ/mol), due to the entropy loss by PA coordination. This unfavorable  $\Delta G$  value explains the presence of an induction period in the early stage of PA polymerization with the catalyst.<sup>13</sup> Another reason for the lower stability of 3B in comparison to 3A is loss of the overlap between the Rh d orbital and Ph  $\pi$  orbital of the triphenylvinyl group of 3A, which is mentioned above. The third reason is the steric repulsion between the phenyl group of the coordinating monomer and nbd moiety of 3B, which is understood from the capture of the conformation shown in the Supporting Information (p S36). It is also possible for a THF molecule to coordinate to the Rh center at the vacant site of 3A, as illustrated in Scheme 4. In fact, the  $\Delta H$  and  $\Delta G$  values from 3A to 3B are +17.5 and +65.0 kJ/mol, while those for THF

coordination to **3A** are  $-3.4$  and  $+38.0$  kJ/mol in THF, respectively.

Scheme 4. Coordination of THF to **3A**



Then, the PA is inserted between the Rh and vinylic carbon atom to give **3C** via the metallacyclobutane transition state **3TS(B-C)**. In this step, 2,1-insertion is preferred to 1,2-insertion, because the  $\pi$  orbital of the benzene ring of PA significantly interacts with the d orbital of Rh during 2,1-insertion to stabilize the transition state, while it does not during 1,2-insertion.<sup>12</sup> PA is inserted in a cis manner, as commonly observed in acetylene polymerization with Rh catalysts, consistent with the cyclobutane transition state **3TS(B-C)**. The activation energies were calculated to be  $\Delta H^\ddagger = 29.3$  kJ/mol and  $\Delta G^\ddagger = 39.8$  kJ/mol from **3B**. The transformation from **3B** to **3C** is largely exothermic ( $\Delta H = -146.1$  kJ/mol,  $\Delta G = -132.8$  kJ/mol), because PA is inserted and a new C–C  $\sigma$  bond is created while a weaker  $\pi$  bond of the alkyne is lost. This is energetically quite favorable and is the reason why polymerization of PA is exothermic. Another reason is extension of conjugation from Rh–C(Ph)=CPh<sub>2</sub> to Rh–C(Ph)=CHC(Ph)=CPh<sub>2</sub>, which is supported by the lower  $\Delta H$  and  $\Delta G$  values of **3C** in comparison to those of **3A**.

The other possible reason for the high stability of **3C** in comparison to **3A** and **3B** is through-space electron donation from the phenyl group to the Rh center, as shown in Figure 6, right. In this case, the  $\gamma$ -phenyl group participates in orbital overlap with Rh in a manner different from the case for **3A**. The distances between the Rh atom and the centers of the  $\beta$ - and  $\gamma$ -phenyl groups are 3.29 and 2.90 Å for **3A** and **3C**, respectively. A Rh–phenyl interaction can exist even though these distances are longer than those of  $\eta^6$ -phenyl–Rh complexes (X-ray crystallographic data 1.8–1.9 Å),<sup>14</sup> and **3C** is more stabilized by the through-space interaction than **3A**. Commonly in Rh-catalyzed polymerizations, PA derivatives are more polymerizable than acetylene monomers having no phenyl group on the acetylene triple bond. The Rh– $\gamma$ -phenyl through-space interaction is possible throughout the propagation process, as long as the monomer insertion takes place in a cis manner. Thus, the high polymerizability of PA derivatives is explained by this interaction as well as the high coordination ability due to the conjugation of the triple bond and the phenyl group. The absence of an induction period during the polymerization of the second monomer feed can also be understood from this mechanistic aspect. The reaction is already in the propagation process when the second feed is added.

As shown in Scheme 3, the second PA (blue) coordinates to the Rh center of **3C** at the site next to the nbd double bond without substituting  $-(\text{CH}_2)_4\text{PPh}_2$  to give **3D**. This process is endothermic ( $\Delta H = +37.5$  kJ/mol,  $\Delta G = +87.1$  kJ/mol), showing a trend similar to, although larger in magnitude, the analogous step from **3A** to **3B**. This result provides support for the larger through-space interaction between Rh and the  $\gamma$ -phenyl group in **3C** in comparison to the Rh and the  $\beta$ -phenyl

group of **3A** mentioned above. The second monomer insertion takes place via the metallacyclobutane transition state **3TS(D-E)** to give **3E** in a similar fashion with the first monomer insertion. After that, the third PA monomer coordinates to the Rh center of **3E** to give **3F**, and successive PA coordination–insertion reactions give poly(PA) having  $-\text{C}(\text{Ph})=\text{CPh}_2$  and a Rh residue at the chain ends. The chain end Rh is converted into H upon addition of acetic acid.<sup>6c</sup>

**Polymerization of PA Derivatives.** The vinyl catalyst **3** was also used for the polymerization of PAs substituted with trimethylsilyl (TMS), *t*-Bu, and F at the para positions. As given in Table 4, monomers bearing *p*-TMS and *p*-*t*-Bu groups

Table 4. Polymerization of PA Derivatives HC≡CC<sub>6</sub>H<sub>4</sub>-*p*-R' with Rh Catalyst **3**<sup>a</sup>

R'	conversion <sup>b</sup> (%)	polymer		
		yield <sup>c</sup> (%)	$M_n^d$	$M_w/M_n^d$
TMS	92	91	75,000	2.2
<i>t</i> -Bu	76	74	45,000	1.6
F	44	40	35,000	1.7

<sup>a</sup>Conditions:  $[\text{M}]_0 = 0.50$  M,  $[\text{M}]_0/[\text{Rh}] = 500$  in THF, 30 °C, 24 h. <sup>b</sup>Determined by GC (*tert*-butylbenzene] = 50 mM as an internal standard). <sup>c</sup>MeOH-insoluble part. <sup>d</sup>Estimated by GPC (polystyrene standard).

underwent polymerization to give the corresponding polymers in good yields (91 and 74%), while the monomer bearing *p*-F gave the polymer in a low yield (40%). It is proposed that the low reactivity of the last monomer is caused by the low coordination ability of the triple bond due to the electron-withdrawing character of F and the low through-space interaction between the Rh center and the phenyl group at the inserted monomer unit.

## CONCLUSIONS

We have developed novel Rh complexes ligated with nbd linked to a phosphino or amino group. These complexes showed catalytic activity for the polymerization of PA and its derivatives. Et<sub>3</sub>N was necessary as an additive for catalyst **1**, which has a phosphino group. On the other hand, catalyst **2**, bearing an amino group, polymerized PA without the assistance of Et<sub>3</sub>N. NMR spectroscopic studies and DFT calculations revealed that **1** exists as a mononuclear complex, while **2** exists as dinuclear complexes. It seems that the dinuclear species of **2** is dissociated by the assistance from the amino group to form a 14e mononuclear complex. This species should be active, and it polymerizes PA smoothly in comparison to **1**, in which the Rh is tightly coordinated by the phosphine ligand. Vinyl catalyst **3** polymerized PA in a controlled manner in the late stage and achieved complete consumption of the second monomer feed. Catalyst **3** is the first well-defined Rh complex coordinated by a tridentate ligand for controlled polymerization of acetylene monomers.

## EXPERIMENTAL SECTION

**Instruments.** Monomer conversions were determined by GC (Shimadzu GC-14B, capillary column (CBP10-M25–025)): column temperature 125 °C, injection temperature 250 °C, flame-ionization detector, internal standard *tert*-butylbenzene. Number- and weight-average molecular weights ( $M_n$  and  $M_w$ , respectively) and polydispersity indices ( $M_w/M_n$ ) of polymers were measured by SEC with a JASCO PU-980/RI-930 chromatograph: 40 °C, eluent THF, columns

KF-805 (Shodex)  $\times$  3, molecular weight limit up to  $4 \times 10^6$ , flow rate 1 mL/min, calibrated with polystyrene standards.  $^1\text{H}$  NMR spectra (400 MHz),  $^{13}\text{C}$  NMR (100 MHz), and  $^{31}\text{P}$  NMR (161 MHz) were recorded on a JEOL EX-400 spectrometer with chemical shifts referenced to the internal standards  $\text{CDCl}_3$  (7.24 ppm for  $^1\text{H}$  NMR),  $\text{CD}_2\text{Cl}_2$  (5.32 ppm, for  $^1\text{H}$  NMR),  $\text{CDCl}_3$  (77.0 ppm for  $^{13}\text{C}$  NMR), and  $\text{CD}_2\text{Cl}_2$  (53.0 ppm, for  $^{13}\text{C}$  NMR) and the external standard  $\text{P}(\text{OMe})_3$  (140 ppm, for  $^{31}\text{P}$  NMR).  $^{103}\text{Rh}$  NMR spectra (12.6 MHz) were recorded on a JNM-ECX400 spectrometer with chemical shifts referenced to the external standard  $\text{Rh}(\text{acac})_3$  (0 ppm). Elemental analyses were performed at the Microanalytical Center of Kyoto University. X-ray crystal structure data were collected on a Rigaku RAXIS RAPID imaging plate area detector with graphite-monochromated Mo  $K\alpha$  radiation ( $\lambda = 0.71075 \text{ \AA}$ ). Crystals of suitable size were mounted on a nylon loop and then transferred to a goniostat for characterization and data collection. The structure was solved by direct methods and expanded using Fourier techniques. All calculations were performed using the crystallographic software package of Rigaku Corp. and Rigaku/MSO CrystalStructure version 3.7.

**Materials.** PA and its derivatives were purchased (Aldrich) and distilled over  $\text{CaH}_2$  under reduced pressure before use.  $\text{KPPH}_2$  (0.5 M in THF, Aldrich) and  $\text{HNPh}_2$  (TCl) were purchased and used without further purification. All solvents were distilled by standard procedures.  $[(\text{C}_2\text{H}_4)_2\text{RhCl}]_2$ <sup>15</sup> and  $\text{nbd}-(\text{CH}_2)_4\text{-Br}$ <sup>16</sup> were synthesized according to the literature.

**Synthesis of  $\text{nbd}-(\text{CH}_2)_4\text{-PPh}_2$ .**  $\text{KPPH}_2$  (0.5 M in THF, 12 mL, 6.0 mmol) was added dropwise to a solution of  $\text{nbd}-(\text{CH}_2)_4\text{-Br}$  (1.30 g, 5.72 mmol) in THF (2.0 mL) under Ar at 0 °C. Then, the mixture was warmed to room temperature and stirred for 1.5 h. Water (0.5 mL) was added to the reaction mixture to quench the reaction, and the resulting mixture was evaporated under vacuum. The residual yellow oil was purified by silica gel column chromatography with hexane as eluent under Ar to give  $\text{nbd}-(\text{CH}_2)_4\text{-PPh}_2$  as a colorless oil (1.41 g, 79%).  $^1\text{H}$  NMR ( $\text{CDCl}_3$ ):  $\delta$  7.42–7.25 (m, 10H), 6.70 (s, 2H), 6.07 (s, 1H), 3.45 (s, 1H), 3.23 (s, 1H), 2.20–2.16 (m, 2H), 2.07–2.02 (m, 2H), 1.92–1.89 (br s, 2H), 1.57–1.49 (m, 2H), 1.44–1.36 (m, 2H).  $^{13}\text{C}$  NMR ( $\text{CDCl}_3$ ):  $\delta$  158.3, 143.7, 142.3, 139.0, 138.9, 133.5, 132.7, 132.5, 128.3, 73.4, 53.3, 49.9, 31.0, 28.8, 27.8, 25.4.  $^{31}\text{P}$  NMR ( $\text{CDCl}_3$ ):  $\delta$  –15.5. Anal. Calcd for  $\text{C}_{23}\text{H}_{25}\text{P}$ : C, 83.10; H, 7.58. Found: C, 83.11; H, 7.58.

**Synthesis of  $\text{nbd}-(\text{CH}_2)_4\text{-NPh}_2$ .**  $\text{NaH}$  (540 mg, 22.5 mmol) was added to a solution of  $\text{nbd}-(\text{CH}_2)_4\text{-Br}$  (520 mg, 2.29 mmol) and  $\text{HNPh}_2$  (1.37 g, 8.09 mmol) in  $\text{CH}_3\text{CN}$  (10 mL). The resulting mixture was heated at 50 °C for 20 h. The reaction mixture was cooled to room temperature and then quenched with water (20 mL) and extracted with  $\text{CHCl}_3$  (20 mL  $\times$  3 times). The combined organic phase was dried over anhydrous sodium sulfate. After filtration, the filtrate was concentrated in vacuo. The residue was purified by silica gel column chromatography with hexane/EtOAc 100/1 (v/v) as eluent to give  $\text{nbd}-(\text{CH}_2)_4\text{-NPh}_2$  as a colorless oil (570 mg, 79%).  $^1\text{H}$  NMR ( $\text{CDCl}_3$ ):  $\delta$  7.25–7.15 (m, 10H), 6.71 (s, 2H), 6.10 (s, 1H), 3.68 (m, 2H), 3.47 (s, 1H), 3.24 (s, 1H), 2.20–2.18 (m, 2H), 1.92 (br s, 2H), 1.63–1.42 (m, 4H).  $^{13}\text{C}$  NMR ( $\text{CDCl}_3$ ):  $\delta$  158.6, 145.8, 143.8, 142.3, 133.3, 128.3, 126.7, 126.5, 73.4, 58.3, 53.4, 50.0, 31.3, 30.0, 25.0. Anal. Calcd for  $\text{C}_{23}\text{H}_{25}\text{N}$ : C, 87.57; H, 7.99; N, 4.44. Found: C, 87.41; H, 7.75; N, 4.36.

**Synthesis of  $[\text{nbd}-(\text{CH}_2)_4\text{-PPh}_2]\text{RhCl}$  (1).** A solution of  $\text{nbd}-(\text{CH}_2)_4\text{-PPh}_2$  (103 mg, 0.31 mmol) in  $\text{CH}_2\text{Cl}_2$  (3.0 mL) was added to a solution of  $[(\text{C}_2\text{H}_4)_2\text{RhCl}]_2$  (55 mg, 0.14 mmol) in  $\text{CH}_2\text{Cl}_2$  (4.0 mL) under Ar at room temperature, and the resulting mixture was stirred for 3 h. After the solvent was removed in vacuo, the resulting orange solid was purified by recrystallization from  $\text{CH}_2\text{Cl}_2/\text{Et}_2\text{O}$ . Yield: 95 mg (83%).  $^1\text{H}$  NMR ( $\text{CDCl}_3$ ):  $\delta$  7.79–7.77 (m, 2H), 7.69–7.66 (m, 2H), 7.38 (m, 6H), 5.33 (s, 1H), 5.22 (s, 1H), 3.78 (s, 1H), 3.56 (s, 1H), 3.36 (s, 1H), 2.37–2.07 (m, 4H), 1.76–1.42 (m, 4H), 1.25–1.10 (m, 2H).  $^{31}\text{P}$  NMR ( $\text{CDCl}_3$ ):  $\delta$  23.7 (d,  $J_{\text{Rh-P}} = 166 \text{ Hz}$ ). Anal. Calcd for  $\text{C}_{23}\text{H}_{25}\text{ClPRh}$ : C, 58.68; H, 5.35. Found: C, 58.73; H, 5.36.

**Synthesis of  $[\text{nbd}-(\text{CH}_2)_4\text{-NPh}_2]\text{RhCl}$  (2).** A solution of  $\text{nbd}-(\text{CH}_2)_4\text{-NPh}_2$  (457 mg, 1.45 mmol) in  $\text{CH}_2\text{Cl}_2$  (5.0 mL) was added to

a solution of  $[(\text{C}_2\text{H}_4)_2\text{RhCl}]_2$  (264 mg, 0.68 mmol) in  $\text{CH}_2\text{Cl}_2$  (8.0 mL) under Ar at room temperature, and the resulting mixture was stirred overnight. After the solvent was removed in vacuo, the orange residue was purified by column chromatography ( $\text{Al}_2\text{O}_3$ ) using toluene as the eluent. The resulting yellow oil was dried in vacuo. Yield: 365 mg (60%).  $^1\text{H}$  NMR ( $\text{CDCl}_3$ ):  $\delta$  7.26–7.21 (m, 4H), 6.99–6.90 (m, 6H), 3.96 (s, 1H), 3.90 (s, 1H), 3.84 (br s, 1H), 3.81 (s, 1H), 3.75–3.69 (m, 3H), 3.51–3.49 (m, 2H), 2.17–2.03 (m, 2H), 1.74–1.55 (m, 4H).  $^{103}\text{Rh}$  NMR ( $\text{CD}_2\text{Cl}_2$ ):  $\delta$  –7052, –7090 ppm. Anal. Calcd for  $\text{C}_{23}\text{H}_{25}\text{NClRh}$ : C, 60.87; H, 5.55; N, 3.09. Found: C, 60.86; H, 5.54; N, 3.03.

**Synthesis of  $[\text{nbd}-(\text{CH}_2)_4\text{-PPh}_2]\text{Rh}(\text{Ph})\text{C}=\text{CPh}_2$  (3).**  $\text{BrMg}\{\text{C}(\text{Ph})=\text{CPh}_2\}$  (0.58 M in THF), was prepared from Mg (0.60 g, 24.7 mmol) with triphenylvinyl bromide (4.19 g, 12.5 mmol) in THF (12 mL), and a portion (0.65 mL, 0.38 mmol) was added to a solution of Rh complex 1 (60 mg, 0.13 mmol) in THF (1.0 mL) under Ar. The resulting mixture was stirred at 50 °C for 24 h. It was concentrated, and the residue was purified by  $\text{Al}_2\text{O}_3$  column chromatography with  $\text{Et}_2\text{O}$  as eluent, followed by recrystallization from  $\text{CH}_2\text{Cl}_2/\text{pentane}$  to give a yellow solid. Yield: 45 mg (51%).  $^1\text{H}$  NMR ( $\text{CD}_2\text{Cl}_2$ ):  $\delta$  8.01–7.97 (m, 2H), 7.52–6.47 (m, 23H), 4.37 (s, 1H), 4.00–3.59 (m, 4H), 3.08–3.01 (m, 2H), 2.48–2.28 (m, 2H), 1.90 (m, 2H), 1.67–1.25 (m, 4H), 1.76–1.42 (m, 4H), 1.25–1.10 (m, 2H).  $^{31}\text{P}$  NMR ( $\text{CD}_2\text{Cl}_2$ ):  $\delta$  26.3. Anal. Calcd for  $\text{C}_{43}\text{H}_{40}\text{PRh}$ : C, 74.78; H, 5.84. Found: C, 74.65; H, 5.91.

**Polymerization.** All the polymerizations were carried out in a Schlenk tube equipped with a three-way stopcock under Ar. A THF solution of PA ( $c = 1.0 \text{ M}$ ) was added to a catalyst solution ( $[\text{Rh}] = 2.0 \text{ mM}$ ). The resulting mixture was stirred at 30 °C for a set time and poured into a large amount of methanol containing a drop of acetic acid to precipitate the polymer. The product was isolated by filtration with a PTFE membrane (pore size 0.2  $\mu\text{m}$ ) and dried under vacuum to constant weight.

**Computation.** All calculations were performed with the GAUSSIAN 09 program,<sup>17</sup> EM64L-G09 Rev C.01, running on the supercomputer system of the Academic Center for Computing and Media Studies, Kyoto University. The enthalpy ( $H$ ) and Gibbs free energy ( $G$ ) at 298.15 K and 1 atm were calculated by the DFT<sup>18</sup> method with the B3LYP functional<sup>19</sup> in conjunction with the LANL2DZ<sup>20</sup> basis set for Rh and the 6-31G\* basis set for the other elements. In some cases, the integral equation formalism variant (IEFPCM) method was employed for the self-consistent reaction field (SCRF) to take into account solvent effects.<sup>21</sup> The feasibility of transition states was checked by the presence of only one imaginary frequency, with the vibrational mode corresponding to the reaction coordinate. Further, intrinsic reaction coordinate (IRC)<sup>22</sup> calculations were carried out using the geometries of the transition states as the initial structures to confirm the connection with reactants and products.

## ■ ASSOCIATED CONTENT

### ● Supporting Information

A figure giving a potential map for Scheme 3 under vacuum, Cartesian coordinates for stationary points of the compounds shown in Schemes 1, 3, and 4, and crystallographic data for 3. This material is available free of charge via the Internet at <http://pubs.acs.org>.

## ■ AUTHOR INFORMATION

### Corresponding Author

\*E-mail: [mshiotsuki@moleng.fuk.kindai.ac.jp](mailto:mshiotsuki@moleng.fuk.kindai.ac.jp) (M.S.); [sanda.fumio.5n@kyoto-u.ac.jp](mailto:sanda.fumio.5n@kyoto-u.ac.jp) (F.S.).

### Notes

The authors declare no competing financial interest.

## ACKNOWLEDGMENTS

This research was supported by a Grant-in-Aid for Scientific Research from the Japan Society for Promotion of Science (22750108), the Global COE Program, "International Center for Integrated Research and Advanced Education in Materials Science" from the Ministry of Education, Culture, Sports, Science and Technology of Japan, The Ogasawara Foundation for the Promotion of Science & Engineering, and The Sumitomo Foundation. We are grateful to Prof. Keiji Morokuma at Kyoto University/Emory University for offering the Cartesian coordinates of related compounds, Prof. Kenneth B. Wagener and Dr. Kathryn R. Williams at the University of Florida for their helpful suggestions and comments, and Mr. Osamu Kamo and Mr. Keiichi Yoshida at JEOL RESONANCE Inc. for measuring the  $^{103}\text{Rh}$  NMR spectra.

## REFERENCES

- (1) Reviews: (a) Choi, S.-K.; Gal, Y.-S.; Jin, S.-H.; Kim, H. K. *Chem. Rev.* **2000**, *100*, 1645–1681. (b) Nagai, K.; Masuda, T.; Nakagawa, T.; Freeman, B. D.; Pinnau, I. *Prog. Polym. Sci.* **2001**, *26*, 721–798. (c) Masuda, T.; Sanda, F. Polymerization of Substituted Acetylenes. In *Handbook of Metathesis*; Grubbs, R. H., Ed., Wiley-VCH: Weinheim, Germany, 2003; Vol. 3, Chapter 3.11, pp 375–406. (d) Aoki, T.; Kaneko, T.; Teraguchi, M. *Polymer* **2006**, *47*, 4867–4892. (e) Masuda, T. *J. Polym. Sci., Part A: Polym. Chem.* **2007**, *45*, 165–180. (f) Masuda, T.; Sanda, F.; Shiotsuki, M. Polymerization of Acetylenes. In *Comprehensive Organometallic Chemistry III*; Crabtree, R., Mingos, D. M. P., Eds., Elsevier: Oxford, U.K., 2007; Vol. 11, Chapter 16, pp 557–593. (g) Yashima, E.; Maeda, K.; Iida, H.; Furusho, Y.; Nagai, K. *Chem. Rev.* **2009**, *109*, 6102–6211. (h) Akagi, K. *Chem. Rev.* **2009**, *109*, 5354–5401. (i) Liu, J.; Lam, J. W. Y.; Tang, B. Z. *Chem. Rev.* **2009**, *109*, 5799–5867. (j) Masuda, T.; Shiotsuki, M.; Sanda, F. Product Class 31: Macromolecular Conjugated Polyenes. In *Science of Synthesis. Houben-Weyl Methods of Molecular Transformations*; Siegel, J. S., Tobe, Y., Eds.; Georg Thieme: Stuttgart, New York, 2010; Category 6, Vol. 45b, pp 1421–1439. (k) Shiotsuki, M.; Sanda, F.; Masuda, T. *Polym. Chem.* **2011**, *2*, 1044–1058.
- (2) (a) Saeed, I.; Shiotsuki, M.; Masuda, T. *Macromolecules* **2006**, *39*, 8567–8573. (b) Saeed, I.; Shiotsuki, M.; Masuda, T. *Macromolecules* **2006**, *39*, 8977–8981. (c) Onishi, N.; Shiotsuki, M.; Sanda, F.; Masuda, T. *Macromolecules* **2009**, *42*, 4071–4076. (d) Shiotsuki, M.; Onishi, N.; Sanda, F.; Masuda, T. *Chem. Lett.* **2010**, *39*, 244–245. (e) Shiotsuki, M.; Onishi, N.; Sanda, F.; Masuda, T. *Polym. J.* **2011**, *43*, 51–57.
- (3) Reviews: (a) Sauer, J. *Angew. Chem., Int. Ed.* **1967**, *6*, 16–33. (b) Sauer, J.; Sustmann, R. *Angew. Chem., Int. Ed.* **1980**, *19*, 779–807. (c) Pindur, U.; Lutz, G.; Otto, C. *Chem. Rev.* **1993**, *93*, 741–761.
- (4) Yip, C.; Handerson, S.; Tranmer, G. K.; Tam, W. *J. Org. Chem.* **2001**, *66*, 276–286.
- (5) Miyake, M.; Misumi, Y.; Masuda, T. *Macromolecules* **2000**, *33*, 6636–6639.
- (6) (a) Onitsuka, K.; Yamamoto, M.; Mori, T.; Takei, F.; Takahashi, S. *Organometallics* **2006**, *25*, 1270–1278. (b) Shiotsuki, M.; Kumazawa, S.; Onishi, N.; Sanda, F. *J. Polym. Sci., Part A: Polym. Chem.* **2011**, *49*, 4921–4925. (c) Kumazawa, S.; Rodriguez Castanon, J.; Onishi, N.; Kuwata, K.; Shiotsuki, M.; Sanda, F. *Organometallics* **2012**, *31*, 6834–6842.
- (7) The  $^{103}\text{Rh}$ – $^{15}\text{N}$  coupling constants of N-ligated Rh complexes are less than 21 Hz. See: (a) Bose, K. S.; Abbott, E. H. *Inorg. Chem.* **1977**, *16*, 3190–3193. (b) Meij, R.; Stufkens, D. J.; Vrieze, K. *J. Organomet. Chem.* **1979**, *164*, 353–370. (c) Pergola, R. D.; Cinquantini, A.; Diana, E.; Garlaschelli, L.; Laschi, F.; Luzzini, P.; Manassero, M.; Reposi, A.; Sansoni, M.; Stanghellini, P. L.; Zanella, P. *Inorg. Chem.* **1997**, *36*, 3761–3771. (d) Rentsch, G. H.; Kozminski, W.; von Philipsborn, W.; Asaro, F.; Pellizer, G. *Magn. Reson. Chem.* **1997**, *35*, 904–907.
- (8) Tabata, M.; Yang, W.; Yokota, K. *Polym. J.* **1990**, *22*, 1105–1107.
- (9) Initiation mechanism with Rh–Cl complexes. It is commonly considered that the Rh–C≡CPh species is first formed by the reaction of the Rh–Cl complex with HC≡CPh (monomer), and then a monomer molecule is inserted into the Rh–C bond to initiate polymerization. However, the mechanism for initiation is still controversial and could potentially include Rh–hydride and Rh–vinylidene species. The necessity of a prereaction prior to the initiation is one possible reason for the activity of **1** being lower than that of **3**. See: (a) Kishimoto, Y.; Eckerle, P.; Miyatake, T.; Ikariya, T.; Noyori, R. *J. Am. Chem. Soc.* **1994**, *116*, 12131–12132. (b) Jiménez, M. V.; Pérez-Torrente, J. J.; Bartolomé, M. L.; Vispe, E.; Lahoz, F. J.; Oro, L. A. *Macromolecules* **2009**, *42*, 8146–8156.
- (10) The energies in the absence of a solvent were also calculated and depicted in Figure S1 (Supporting Information). The difference between the energies in THF and vacuum for each intermediate was  $\pm 0.9$ –14.1 kJ/mol.
- (11) Kishimoto, Y.; Eckerle, P.; Miyatake, T.; Kainosho, M.; Ono, A.; Ikariya, T.; Noyori, R. *J. Am. Chem. Soc.* **1999**, *121*, 12035–12044.
- (12) Ke, Z.; Abe, S.; Ueno, T.; Morokuma, K. *J. Am. Chem. Soc.* **2011**, *133*, 7926–7941.
- (13) The transformation from **3** to **3B** via **3A** possibly accompanies reverse reactions, because the coordination of Rh with PA and PPh<sub>3</sub> is competitive. The polymerization of PA with [(nbd)RhCl]<sub>2</sub>/BuLi/PPh<sub>3</sub> is retarded progressively with increasing PPh<sub>3</sub> concentration. See: Kanki, K.; Misumi, Y.; Masuda, T. *Macromolecules* **1999**, *32*, 2384–2386.
- (14) (a) Onishi, N.; Shiotsuki, M.; Sanda, F.; Masuda, T. *Macromolecules* **2009**, *42*, 4071–4076. (b) Liu, Z.; Yamamichi, H.; Madrahimov, S. T.; Hartwig, J. F. *J. Am. Chem. Soc.* **2011**, *133*, 2772–2782. (c) Shi, Y.; Blum, S. A. *Organometallics* **2011**, *30*, 1776–1779. (d) Grochowski, M. R.; Morris, J.; Brennessel, W. W.; Jones, W. D. *Organometallics* **2011**, *30*, 5604–5610. (e) Hooper, J. F.; Chaplin, A.; González-Rodríguez, C.; Thompson, A. L.; Weller, A. S.; Willis, M. C. *J. Am. Chem. Soc.* **2012**, *134*, 2906–2909. (f) Chaplin, A. B.; Hooper, J. F.; Weller, A. S.; Willis, M. C. *J. Am. Chem. Soc.* **2012**, *134*, 4885–4897.
- (15) Cramer, R.; McCleverty, J. A.; Bray, J. *Inorg. Synth.* **1974**, *15*, 14–18.
- (16) Yip, C.; Handerson, S.; Tranmer, G. K.; Tam, W. *J. Org. Chem.* **2001**, *66*, 276–286.
- (17) Frisch, M. J.; Trucks, G. W.; Schlegel, H. B.; Scuseria, G. E.; Robb, M. A.; Cheeseman, J. R.; Scalmani, G.; Barone, V.; Mennucci, B.; Petersson, G. A.; Nakatsuji, H.; Caricato, M.; Li, X.; Hratchian, H. P.; Izmaylov, A. F.; Bloino, J.; Zheng, G.; Sonnenberg, J. L.; Hada, M.; Ehara, M.; Toyota, K.; Fukuda, R.; Hasegawa, J.; Ishida, M.; Nakajima, T.; Honda, Y.; Kitao, O.; Nakai, H.; Vreven, T.; Montgomery, J. A., Jr.; Peralta, J. E.; Ogliaro, F.; Bearpark, M.; Heyd, J. J.; Brothers, E.; Kudin, K. N.; Staroverov, V. N.; Keith, T.; Kobayashi, R.; Normand, J.; Raghavachari, K.; Rendell, A.; Burant, J. C.; Iyengar, S. S.; Tomasi, J.; Cossi, M.; Rega, N.; Millam, J. M.; Klene, M.; Knox, J. E.; Cross, J. B.; Bakken, V.; Adamo, C.; Jaramillo, J.; Gomperts, R.; Stratmann, R. E.; Yazyev, O.; Austin, A. J.; Cammi, R.; Pomelli, C.; Ochterski, J. W.; Martin, R. L.; Morokuma, K.; Zakrzewski, V. G.; Voth, G. A.; Salvador, P.; Dannenberg, J. J.; Dapprich, S.; Daniels, A. D.; Farkas, O.; Foresman, J. B.; Ortiz, J. V.; Cioslowski, J.; Fox, D. J. *Gaussian 09, Revision C.01*; Gaussian, Inc., Wallingford, CT, 2010.
- (18) Parr, R. G.; Yang, W. *Density-Functional Theory of Atoms and Molecules*; Oxford University Press: Oxford, U.K., 1989.
- (19) (a) Lee, C. T.; Yang, W. T.; Parr, R. G. *Phys. Rev. B* **1988**, *37*, 785–789. (b) Becke, A. D. *J. Chem. Phys.* **1993**, *98*, 5648–5652.
- (20) (a) Dunning, T. H., Jr.; Hay, P. J. In *Modern Theoretical Chemistry*; Schaefer, H. F., III, Ed.; Plenum: New York, 1976; Vol. 3, pp 1–28. (b) Hay, P. J.; Wadt, W. R. *J. Chem. Phys.* **1985**, *82*, 270–283. (c) Wadt, W. R.; Hay, P. J. *J. Chem. Phys.* **1985**, *82*, 284–298. (d) Hay, P. J.; Wadt, W. R. *J. Chem. Phys.* **1985**, *82*, 299–310.
- (21) Tomasi, J.; Mennucci, B.; Cammi, R. *Chem. Rev.* **2005**, *105*, 2999–3093.
- (22) Fukui, K. *Acc. Chem. Res.* **1981**, *14*, 363–368.